Palate Lung Nasal Clone (PLUNC), a Novel Protein of the Tear Film: Three-Dimensional Structure, Immune Activation, and Involvement in Dry Eye Disease (DED)

Martin Schicht,[1] Felix Rausch,[1] Martin Beron,[1] Christina Jacobi,[2] Fabian Garreis,[1] Nadine Hartjen,[1] Stephanie Beileke,[1] Friedrich Kruse,[2] Lars Bräuer,[1] and Friedrich Paulsen[1]

[1]Department of Anatomy II, Friedrich-Alexander-University Erlangen-Nürnberg, Erlangen, Germany
[2]Department of Ophthalmology, Friedrich-Alexander-University Erlangen-Nürnberg, Erlangen, Germany

Correspondence: Martin Schicht, Department of Anatomy II, University of Erlangen-Nürnberg, Universitätsstraße 19, 91054 Erlangen, Germany; martin.schicht@anatomie2.med.uni-erlangen.de, friedrich.paulsen@fau.de.

MS and FR contributed equally to the work presented here and should therefore be regarded as equivalent authors.

LB and FP contributed equally to the work presented here and should therefore be regarded as equivalent authors.

Submitted: June 24, 2015
Accepted: September 20, 2015

Citation: Schicht M, Rausch F, Beron M, et al. Palate lung nasal clone (PLUNC), a novel protein of the tear film: three-dimensional structure, immune activation, and involvement in dry eye disease (DED). *Invest Ophthalmol Vis Sci*. 2015;56:7312–7323. DOI:10.1167/iovs.15-17560

Purpose. Palate Lung Nasal Clone (PLUNC) is a hydrophobic protein belonging to the family of surfactant proteins that is involved in fluid balance regulation of the lung. Moreover, it is known to directly act against gram-negative bacteria. The purpose of this study was to investigate the possible expression and antimicrobial role of PLUNC at the healthy ocular surface and in tears of patients suffering from dry eye disease (DED).

Methods. Bioinformatics and biochemical and immunologic methods were combined to elucidate the structure and function of PLUNC at the ocular surface. Tissue-specific localization was performed by using immunohistochemistry. The PLUNC levels in tear samples from non-Sjögren's DED patients with moderate dry eye suffering either from hyperevaporation or tear deficiency were analyzed by ELISA and compared with tears from healthy volunteers.

Results. Palate Lung Nasal Clone is expressed under healthy conditions at the ocular surface and secreted into the tear film. Protein modeling studies and molecular dynamics simulations performed indicated surface activity of PLUNC. In vitro experiments revealed that proinflammatory cytokines and bacterial supernatants have only a slight effect on the expression of PLUNC in HCE and HCjE cell lines. In tears from DED patients, the PLUNC concentration is significantly increased (7-fold in evaporative dry eye tears and 17-fold in tears from patients with tear deficiency) compared with healthy subjects.

Conclusions. The results show that PLUNC is a protein of the tear film and suggest that it plays a role in fluid balance and surface tension regulation at the ocular surface.

Keywords: PLUNC1, BPIFA1, SPURT, LUNX, NASG, ocular surface, dry eye disease (DED), tear film, surfactant protein

The ocular surface is regularly exposed to an array of microbes, bacterial components, and their pathogen-associated molecular patters. It is therefore important to understand the mechanisms by which the ocular surface epithelia and their products protect the host from infection and/or colonization by invading microorganisms. The ocular surface epithelia serve as a vital barrier separating microbial invaders from underlying tissues, while the constant tear flow and the movement of the tear film through blinking facilitates clearance of bacteria, viruses, and other particles in the process of fluid-flow clearance. Additionally, the tear fluid contains many factors cooperating to prevent potential pathogens from getting a foothold at the ocular surface. Tear fluid contains a number of secreted innate immune molecules with defined host defense roles, including classical antimicrobial proteins, such as lysozyme and lactoferrin, as well as antimicrobial peptides, such as the defensins, LL37, and others.[1] In addition, tear fluid contains many factors that contribute to other aspects of host defense or to tear film homoeostasis, such as mucins, electrolytes, and surfactants.

Proteins with surfactant activity have just recently been described as part of the ocular surface and tear film.[2,3] Comparable to their functions in the lung, surfactant proteins (SP)-B and SP-C have been suggested to operate in association with lipids of the tear film to break the surface tension of the tear film, which will be particularly important to prolong tear film break-up time.[3] The other two, SP-A and SP-D, do not show significant surface activity in the lung, but are innate immune defense lectins of the collectin family. They are also part of the ocular surface and tear film and have been suggested to have here similar functions as in the lung.[2,4] However, SPs have not yet been quantified in tear fluid and due to a lack of functional studies, the action of these four surfactant proteins within the tear film are a particularly poorly understood aspect of ocular surface innate immunity.

Interestingly, in airway surface liquid lining the upper respiratory tract, SP-B and SP-C are notably absent or nearly absent.[5,6] Instead, the Palate Lung Nasal Clone (PLUNC) protein is among the most abundant products in these airway secretions.

Palate Lung Nasal Clone, also known as SPLUNC1 (S = secreted), PLUNC1, LUNX (lung-specific X protein), NASG (nasopharyngeal carcinoma-related protein), or SPURT (secretory protein in upper respiratory tracts) is a secreted glycoprotein of approximately 25 kDa that is an important protein involved in innate immunity.[7] It is highly expressed in healthy airways, goblet cells, and minor mucosal glands of the respiratory tract and oral cavity, surface epithelium ciliated cells, and human submucosal gland serous cells,[8,9] and with that at sites of great environmental exposure. Because of its physicochemical properties (distinct hydrophobicity) and cellular distribution, PLUNC belongs to the family of surfactant proteins and significantly contributes to the overall surface tension in airway epithelial secretions.[7] Moreover, physiologically relevant concentrations of PLUNC inhibited *Pseudomonas aeruginosa* biofilm formation without acting directly as a bactericide.[10] By inhibition of sodium channels (ENaC) in the lung, PLUNC can directly influence the fluid balance of the lung.[11] The data so far available about PLUNC reveal a multifunctional protein, which plays a novel role in airway defense at the air/liquid interface. Thus, PLUNC has been shown to be induced and upregulated during microbial infection[12] and its expression is also upregulated after neuronal injury.[13] In cases of cystic fibrosis, PLUNC is also upregulated. However, it is unclear whether the observed increase in protein expression plays any role in the pathogenesis of the disease.[14]

Based on this information about PLUNC, we tested in the present study the hypothesis of whether human PLUNC is also part of the lacrimal system and might here have functions similar to the known functions in the lung. As a structure model of PLUNC did not exist when starting these studies, we also conducted protein modeling studies and molecular dynamics simulations to learn more about the possible surface activity of PLUNC.

Materials and Methods

Tissues

The tissue samples were obtained from cadavers (5 male, 11 female, aged 33–76 years) donated to the Department of Anatomy and Cell Biology, Martin Luther University Halle-Wittenberg, Germany. The study was approved by the institutional review board of the Martin Luther University Halle-Wittenberg in accordance with the Declaration of Helsinki. The used samples were dissected from the cadavers within a time frame of 5 to 20 hours post mortem. Previous to dissection, the history of each cadaver was studied. The donors were free of recent trauma, eye and nasal infections, or diseases involving or affecting lacrimal function. Moreover, with regard to the whole body, donors that were affected by acute infection, tumors, recent trauma, or surgical operations were not used in this study. After dissection of cornea, conjunctiva, lacrimal gland, eyelid, and efferent tear ducts (lacrimal sac and nasolacrimal duct), respectively, half of each specimen was fixed in 4% paraformaldehyde for later paraffin embedding. The other half of each sample was used for molecular–biological investigations and thus was immediately frozen at –80°C. Bronchial mucosa and lung samples served as positive control tissues.

Tear Fluid

Tear fluid samples ($n = 39$; mean age 55.9 ± 13.2 years: 20 women, 19 men) were collected at the Department of Ophthalmology, Friedrich-Alexander-University Erlangen-Nürnberg, Germany. Here, they were obtained in compliance with good clinical practice and with informed consent. Ethical approval was obtained from the Ethics Committee of the University of Erlangen-Nürnberg. Written consent was obtained from all patients and subjects after explanation of the procedures and study requirements. Tears from 21 control subjects (mean age 42.8 ± 8.3 years; 9 women and 13 men) were included in the study. They had no symptoms for DED or ocular discomfort, did not use any artificial tears or lubricant eye drops, and did not suffer from any autoimmune disorders or other eye diseases including ocular allergies and had no history of eye surgery or contact lens wearing. Thirty-nine eyes of 39 patients (mean age 42.8 ± 8.3 years; 20 women and 19 men) with moderate to severe dry eye (DEWS, dry eye severity level 2)[15] were enrolled in the study. Inclusion criteria were typical symptoms measured by a validated questionnaire: Ocular Surface Disease Index questionnaire Score (OSDI Score) > 40, a tear break-up time (TBUT) ≤ 10 seconds, a Schirmer test with anesthesia ≤ 10 mm, and lid-parallel conjunctival folds (LIPCOF) > 2. Patients were divided into two subgroups: evaporative dry eye (EDE, $n = 25$) and aqueous-deficient dry eye (ADDE, $n = 14$). The EDE patients had a TBUT of ≤ 5 seconds and a Schirmer test ≤ 10 mm. The ADDE patients showed a TBUT of ≤ 10 seconds and a Schirmer test ≤ 5 mm. Exclusion criteria consisted of a medical history of trauma or infection, ocular allergies, pregnancy, lactation, history of refractive surgery/ocular surgery/any other surgery within the previous 6 months, immunosuppressive medications, or the use of contact lenses within 14 days before ophthalmologic examination. Moreover, patients wearing punctum plugs; patients with history or evidence of epithelial keratitis from herpes simplex; recent varicella; corneal or conjunctival viral disease; acute corneal, conjunctival, or palpebral bacterial infection; or ocular fungal infection were excluded from this study.

The following test measurements were accomplished with all patients.

The OSDI Score Questionnaire. The OSDI is a subjective symptom questionnaire that measures the severity of DED. It includes 12 items regarding visual function, ocular symptoms, and environmental triggers queried for the past week. Possible answers for the questions are as follows: none of the time, some of the time, half of the time, most of the time and all of the time (0–4). The scoring algorithm published contains scores from 0 to 100.[16] The OSDI is used as an outcome measure in randomized controlled trials.[17]

Lid-Parallel Conjunctival Folds (Degree 0–3). Lid-parallel conjunctival folds were evaluated by slit-lamp examination. The classification of LIPCOF according to Höh et al.[18] was used. With degree 0, no permanent conjunctival fold exists. Degree 1 describes the permanent presence of an individual fold, which does not exceed the height of the normal tear meniscus. With degree 2, the LIPCOF disintegrates into two or several small parallel folds that are lower than the normal tear meniscus. If there are several parallel conjunctival folds exceeding the height of the normal tear meniscus, then degree 3 exists.

Tear Break-Up Time(s). For diagnosing tear film stability, a standardized measurement of the tear film break-up time was accomplished. A total of 5 µL nonpreserved 2% sodium fluorescein was instilled onto the bulbar conjunctiva without inducing reflex tearing by using a micropipette. Then the patient was instructed to blink normally without squeezing several times to distribute the fluorescein and then refrain from blinking until told otherwise. The slit-lamp magnification was set at ×10 and a Wratten 12 yellow filter was used to enhance observation of the tear film over the entire cornea.[19] A stopwatch was used to record time between last complete

blink and the first disruption of the tear film. After observing the TBUT, the patient was instructed to blink normally again. Three measurements were taken as recommended by the DEWS report 2007,[15] and the average was calculated.

Schirmer Test With Anesthesia (Eyes Closed, mm). After topical anesthesia with one drop oxybuprocaine-HCL (Conjuncain-EDO), a Schirmer test strip (35 × 5 mm; Liposic-Schirmer-Test-Streifen, Dr Mann Pharma, Berlin, Germany) was placed in the lower outer fornix and then the patient was instructed to close his or her eyes. After 5 minutes, the strip was removed from the eye and the length of wetting was measured.[17] In addition, the tear fluid–soaked Schirmer strip was transferred to a 1.5-mL reaction tube and stored at –80°C for further testing.

Isolation of the Tear Fluid From Schirmer Strips

For extraction of the tear fluid, the Schirmer strips were transferred to a 0.5-mL tube punctured at the bottom with a cannula. The tube was placed in a larger (1.5 mL) tube and centrifuged at 13,000*g* (17,900 rct) for 5 minutes. The centrifugal force pulled the tear fluid out of the Schirmer strip, through the central "pore" in the bottom of the smaller tube and into the outer 1.5 mL tube.[20]

Cell Culture

The SV40-transformed human corneal epithelial cells (HCE cells, obtained from Kaoru Araki-Sasaki, Tane Memorial Eye Hospital, Osaka, Japan, passage number 18-27),[21] as well as a human spontaneously immortalized epithelial cell line from normal human conjunctiva (IOBA-NHC, here referred to as human conjunctiva epithelial cell line [HCjE] cells, obtained from Yolanda Diebold, University Institute of Applied Ophthalmobiology [IOBA], University of Valladolid, Valladolid, Spain)[22] were cultured as monolayer and used for further stimulation experiments. The HCE and HCjE cells were cultured with Dulbecco's modified Eagle's medium (DMEM)/HAM's F12 (1:1; PAA Laboratories GmbH, Pasching, Austria) supplemented with 10% fetal calf serum (Biochrom AG, Berlin, Germany) in a humidified 5% CO_2 incubator at 37°C. For stimulation experiments, cells (1×10^6) were seeded in Petri dishes and cultured until confluence was reached. Cells were washed with PBS and changed to serum-free mediums for 3 hours. Afterward, cells were treated with recombinant proinflammatory cytokine IL-1β (10 ng/mL; ImmunoTools, Friesoythe, Germany), TNF-α (10 ng/mL; ImmunoTools), lipopolysaccharide (LPS; 100 ng/mL) for 6, 12, 24, or 48 hours each, or with different dilutions of bacterial supernatants of *Escherichia coli* (EC) or *Pseudomonas aeruginosa* (PA) for 6, 24, or 48 hours. In each experiment, supernatants of bacterial cells were incubated with Tryptone Soy Broth (TSB) medium as a control or in case of proinflammatory cytokines stimulated with the cytokine solvent. All experimental procedures were performed under normoxic conditions. On completion of each experiment, cells and culture supernatants were collected and stored at –80°C until they were processed for RNA extraction (cells) or analysis of PLUNC secretion (culture supernatants) by ELISA experiments.

Production of Bacterial Supernatants

Laboratory strains of *P. aeruginosa* PAO1 (ATCC 15692) and *E. coli* (ATCC 8739) were grown overnight at 37°C by shaking in TSB (Oxoid, Basingstoke, England). Bacteria were centrifuged twice at 6000 rpm for 30 minutes. Supernatants were filtered twice using filters impermeable to bacteria (0.22-μm pore size; Millipore, Eschborn, Germany). Aliquots of the supernatants were proven to be sterile by overnight incubation on agar. The TSB growth medium (diluted 1:100) served as medium control.

Preparation of RNA and cDNA Synthesis

For conventional RT-PCR, tissue biopsies were crushed in an agate mortar under liquid nitrogen and homogenized (Polytron, Norcross, GA). Total RNA was extracted from the samples by RNeasy Mini Kit (Qiagen, Hilden, Germany).

In addition, total RNA was extracted from cultivated HCE and HCjE (PeqGold reagent; PeQLab, Erlangen, Germany). Crude RNA was purified with isopropanol and repeated ethanol precipitation, and contaminated DNA was destroyed by digestion with RNase-free DNase I (30 minutes, 37°C; Boehringer, Mannheim, Germany). The DNase was heat-inactivated for 10 minutes at 65°C. Reverse transcription of all RNA samples to first-strand cDNA (RevertAid H Minus M-MuL V Reverse Transcriptase Kit; Fermentas, St. Leon-Rot, Germany) was performed according to the manufacturer's protocol. Two micrograms total RNA and 10 pmol Oligo $(dT)_{18}$ primer (Fermentas) were used for each reaction. The ubiquitously expressed β-actin and HPRT, which proved amplifiable in each case with the specific primer pair, served as the internal control for the integrity of the translated cDNA.

Polymerase Chain Reaction (RT-PCR)

For conventional PCR, we used conditions as previously described with the following primers: PLUNC sense 5′-AGG TCT TCT GGA CAG CCT CA-3′, antisense 5′-CTG TAG TCC GTG GAT CAG CA-3′ (approximately 275 bp), and PLUNC real sense 5′-CGG AGA GAA GGC AAC TGT GT-3′, antisense 5′-CAT CAA GGT CTA AGC CTT CCA-3′ (approximately 90 bp).[23] The PCR products were also confirmed by BigDye sequencing (Applied Biosystems, Foster City, CA, USA). To estimate the amount of amplified PCR product, we performed a β-actin PCR with specific primers (sense 5′- CAA GAG ATG GCC ACG GCT GCT-3′, antisense 5′-TCC TTC TGC ATC CTG TCG GCA-3′, 275 bp) for each investigated sample. The PCR products were also confirmed by BigDye sequencing (Applied Biosystems).

Quantitative Real-Time RT-PCR

Gene expression was analyzed with a LightCyler480 (Roche Applied Sciences, Basel, Switzerland). Real-time RT-PCR was performed with PLUNC primers (see above) to allow calculation of the relative abundance of transcripts. The PCR reaction contained 10 μL LightCycler480 5× probe mastermix (Roche Applied Sciences), 0.5 μL each primer mix and 2 μL each cDNA, 0.4 μL Universal ProbeLibrary (UPL) probe #11 (10 μM; Roche Applied Sciences), and 7.1 μL nuclease free water. In each plate quantitative PCR was performed with a cycle of 5 minutes 95°C, 55 cycles at 15 seconds 95°C, 30 seconds 60°C, and 1 second 72°C, to confirm amplification of specific transcripts. The PLUNC primers and corresponding UPL probe was performed using the ProbeFinder software (Version 2.04; Roche Applied Sciences). A standard curve was generated by 6-fold serial dilutions of cDNA from nonstimulated cells. To standardize mRNA concentration, the transcript levels of the housekeeping gene small ribosomal subunit (18S rRNA) were determined in parallel for each sample, and relative transcript levels were corrected by normalization based on the 18S rRNA transcript levels. The primers for 18S rRNA were as follows: forward 5′-GGT GCA TGG CCG TTC TTA-3′ and reverse 5′-TGC CAG AGT CTC GTT TA-3′. All real-time RT-PCR analyses were performed

Investigative Ophthalmology & Visual Science

in triplicate, and the changes in gene expression were calculated by the $^{\Delta\Delta}C_t$ method.

Western Blot Analysis

For Western blot, tissue samples (standardized ratio: 100 mg wet weight/400 μm buffer containing 1% SDS and 4% 2-mercaptoethanol) were extracted as previously described.[24] The protein was measured with a protein assay based on the Bradford dye-binding procedure (BioRad, Hercules, CA, USA). The total protein (30 μg) was then analyzed by Western blot. Proteins were resolved by reducing 15% SDS-PAGE, electrophoretically transferred at room temperature for 1 hour at 0.8 mA/cm^2 onto 0.1-μm pore size nitrocellulose membranes. Bands were detected with primary antibody to PLUNC (rabbit-anti-PLUNC, 1:200, SC133917, Santa Cruz Biotechnology, Dallas, TX, USA; goat-anti-PLUNC, 1:200, SC49248, Santa Cruz) and secondary antibody (anti-rabbit IgG, respectively, conjugated to horseradish peroxidase, 1:5000) using chemiluminescence (ECL-Plus; Amersham-Pharmacia, Uppsala, Sweden). Human bronchial tissue was used as control. The molecular weights of the detected protein bands were estimated using standard proteins (Prestained Protein Ladder; Fermentas) ranging from 10 to 170 kDa.

Immunohistochemistry

For immunohistochemistry, tissue specimens from healthy tissues of cadavers were embedded in paraffin, sectioned (6 μm), and dewaxed. Immunohistochemical staining was performed with the polyclonal antibody against PLUNC (rabbit-anti-PLUNC, 1:100, SC133917, Santa Cruz; goat-anti-PLUNC, 1:100, SC49248, Santa Cruz). Antigen retrieval was performed by microwave pretreatment for 10 minutes and nonspecific binding was inhibited by incubation with porcine normal serum (Dako, Glostrup, Denmark) 1:5 in Tris-buffered saline. Each primary antibody (1:50–1:100) was applied overnight at room temperature. The secondary antibodies (1:300) were incubated at room temperature for at least 4 hours. Visualization was achieved with aminoethylcarbazole (AEC) for at least 5 minutes. Red-stained areas within the sections indicate a positive antibody reaction. After counterstaining with hemalum, sections were mounted in Aquatex (Boehringer, Mannheim, Germany). Bronchial epithelium served as positive control. Two negative control sections were used in each case: one was incubated with the secondary antibody only, and the other one with the primary antibody only. The slides were examined with a Keyence Biorevo BZ9000 microscope.

Enzyme-Linked Immunosorbent Assay

The ELISA analysis was performed using a kit for Human Palate/Lung and Nasal Epithelium Associated Protein (PLUNC, E97364; USCN HuLife Science, Inc., Wuhan, China) and the regarding protocols from USCN. The analysis was performed using a microplate spectrophotometer (ELISA reader) at a wavelength of 450 nm and 405 nm for measuring the absorbance from tear fluid samples. By comparing with the standard series and the determined values for antigen concentration (protein concentration), each sample was calculated in ng/mg.

Protein Structure Model Creation

The protein structure model for PLUNC was obtained by the classical comparative modeling approach. Therefore, the homology modeling protocol provided by YASARA[25,26] was used for the human PLUNC amino acid sequence of the UniProt[27] entry Q9NP55. The residues of the signal peptide were removed before the modeling. The recently available x-ray structure of latherin (PDB code "3ZPM")[28] was used as the template structure, as it is already known from the literature that PLUNC and latherin have a sufficient sequence identity of 28% and are members of the same protein family with BPI-like fold.[29] Energy minimizations and MD refinements[26] with YASARA and the YASARA2 force field[26] were performed to further improve the intramolecular interactions and stereochemistry of the resulting model. To assess the model quality, PROCHECK[30] was used to evaluate the stereochemistry and PROSA II[31] was performed to check the quality of the entire protein fold or identify possibly misfolded regions. PROSA II contains knowledge-based mean fields derived from statistical analysis of well-resolved protein x-ray structures. Both validation programs can suggest whether a structure model resembles a native-like fold or not.

The stability of the final protein model was assessed by a 20-ns MD simulation in YASARA with the AMBER03 force field.[32] The simulation was performed with the protein placed in a water box with a physiological NaCl concentration of 0.9% and 298 K temperature. The MD analysis was done with scripts implemented in YASARA to calculate root mean square deviation (RMSD), RMSF, and secondary structure assignment with DSSP.[33] The final PLUNC model was accepted by and deposited at the Protein Model DataBase PMDB (https://bioinformatics.cineca.it/PMDB/, in the public domain) and received the PMDB id PM0079571 for public download.

Molecular Dynamics Simulations

To study possible interactions between the PLUNC protein model and a lipid environment, a plain membrane system consisting solely of the ubiquitous phospholipid dipalmitoylphosphatidylcholine (DPPC) was used. The initial bilayer system consisting of 512 lipid molecules, 256 per layer, was built with the CELLmicrocosmos MembraneEditor 2.2 (Bielefeld University, Bielefeld, Germany).[34] For the simulation start systems, one copy of the protein model was placed in proximity to the preequilibrated membrane, the simulation box was filled with water, and neutralized with Na^+ ions. The orientation of the protein model was slightly altered for different simulation starts, generating seven different starting orientations, whereof in two cases, the 20 N-terminal residues were positioned as transmembrane section. The total size of each resulting simulation system was approximately 206,000 atoms.

The protein–lipid simulations were performed with the GROMACS package version 4.6.1.[35] The united-atom G53a6 force field[36] was modified after Kukol[37] to reproduce experimental literature data for a DPPC-lipid system. After a short equilibration period (500 ps), the simulations for all seven systems were carried out for 100 ns with the Nosé-Hoover thermostat[38,39] at 323 K and the Parrinello-Rahman barostat[40] with semi-isotropic coupling and a reference pressure of 1 bar. Periodic boundary conditions were applied in all three dimensions. The LINCS constraint algorithm[41] was used to fix the bond stretching of all hydrogen involving atom bonds, allowing a simulation time step of 2 fs. Electrostatic interactions were calculated with the Particle Mesh Ewald (PME) algorithm[42] as implemented in GROMACS with the cutoff at 1.2 nm and the van der Waals potential switched off between 1.2 and 1.3 nm. The neighbor list was updated every 10 steps and no dispersion correction was applied. Two energy groups were introduced to obtain the protein–lipid interaction energy during the simulation. The analysis of the simulations was done with the tools integrated in the GROMACS package.

Visualization of the structures and trajectories was done with VMD[43] and YASARA.

Statistical Analysis

Data are expressed as mean ± SEM. As nonparametric statistics, we performed ANOVA (Kruskall-Wallis-Test) test. We compared healthy samples as control between ADDE and EDE. The GraphPad prism 5 for Windows software package (GraphPad, La Jolla, CA, USA) was used for the statistical analysis; $P < 0.05$ was considered statistically significant.

Results

Modeling the Protein Structure of PLUNC

The homology modeling procedure with the x-ray structure of latherin as template structure resulted in a PLUNC structure model that passed the basic YASARA quality checks. Only the first 30 N-terminal residues needed further improvement beside of the standard YASARA MD refinement and energy minimization, as this sequence part was not covered by the template structure. The model contains a disulfide bond bridging the only two cysteine residues at positions 161 and 205, which was adopted from the template structure. The quality evaluation with PROSA suggested a native-like fold of the whole model, with the combined Z-score (–8.07) comparable to the statistical average value for proteins of this length (–10.01). The stereochemical quality assessed by PROCHECK did not indicate any problems, which means that the dihedral angles of 91% of the 237 amino acids were in the most favored regions and the remaining 9% showed angle values in the additional allowed regions of the Ramachandran plot. This resulted in combination with the positive PROSA evaluation suggesting a good quality and native-like fold of the final model, giving first insights into the three-dimensional structure of PLUNC (Fig. 1A).

The stability of the protein model was investigated by a 20-ns MD simulation in a water box with YASARA. The RMSD was used as an indication for the model stability (Fig. 1B). This value describes the distance between the backbone atoms of the final structure in comparison with the simulation start. The RMSD was essentially stable after 8 ns with slightly increased fluctuations in the last 2 ns. Fluctuation analysis for each residue (RMSF, not shown) showed that these instabilities in the RMSD plot are caused by individual short loop sections (17–23, 73–86, and 175–183). Due to their high content of hydrophobic amino acids exposed to the water, they were very flexible during the MD. The core secondary structure elements, however, remained stable during the whole simulation. This was underlined by the protein structure analysis with DSSP, which showed an average α-helix, β-sheet, and random coil content of approximately 32%, 27%, and 41%, respectively, for the first as well as the last 2 ns of the MD simulation. Therefore, the PLUNC model could be considered as stable and the last snapshot of the simulation was used for further MD studies.

PLUNC is Expressed in Tissues of the Ocular Surface and Lacrimal Apparatus and Is Increased in Tears of Patients Suffering From DED

Tissue samples from eyelid, lacrimal gland, conjunctiva, cornea, and lung ($n = 5$ for each tissue) revealed presence of PLUNC mRNA (Fig. 1C). The β-actin control PCR was positive for all samples. The detected PCR bands (130 bp) were in accordance to the expected sequences from PLUNC within the NCBI gene bank data (www.ncbi.com, in the public domain).

Protein extracts from eyelid, lacrimal gland, conjunctiva, cornea and lung ($n = 5$, respectively) as well as five tear fluid samples from healthy volunteers and six samples from patients suffering from DED (3 × EDE and 3 × ADDE were pooled) were tested for presence of PLUNC by means of Western blot analysis (Figs. 1D, 1E). The antibody revealed a distinct protein band for PLUNC at 40 kDa, respectively. Lung tissue, used as a positive control, was treated and incubated at the same conditions as all other samples. Tear fluid from patients suffering from DED revealed a significantly higher PLUNC protein concentration than tears from healthy volunteers (Figs. 1E, 1F).

Paraffin-embedded 6-μm sections from eyelid (including palpebral conjunctiva, meibomian gland, glands of Moll), lacrimal gland, cornea, and efferent tear ducts ($n = 16$, respectively) were analyzed. All investigated tissue samples showed antibody reactivity against PLUNC (Fig. 2). Control sections (primary and secondary antibody only) were negative (unstained) for each tissue. The insets within the figures show magnifications for the respective tissue. For all tissues, red staining revealed positive antibody reactivity for PLUNC. Cornea: PLUNC was only detected in the basal epithelial cell layer of the corneal epithelial cells (Fig. 2A). In addition, also endothelial cells revealed reactivity against the PLUNC antibody (Fig. 2B), whereas the stroma did not react. Lining epithelium of the eyelid: Strong PLUNC reactivity was visible in the basal epithelial cell layer and faint reactivity within the other layers of the epidermis (Fig. 2C). Subepithelial tissue did not reveal reactivity. Conjunctiva: Epithelial cells of the conjunctiva reacted intracytoplasmically positive with the PLUNC antibody with the exception of intraepithelial goblet cells that did not react (Fig. 2D). Lacrimal gland: Reactivity of PLUNC was detected intracytoplasmically within acinar cells (Fig. 2E). Meibomian glands: Meibocytes reacted positive with the PLUNC antibody, as did also the lining cells of the excretory duct system did (Fig. 2F). Glands of Moll: The epithelium of the glands of Moll demonstrated intracytoplasmically antibody reactivity against PLUNC (not shown). Efferent tear ducts: Expression of PLUNC was observed intracytoplasmically in the double-layered epithelium (exception: goblet cells) (Fig. 2G). Strong reactivity was visible on the apical surface of the lining cells. In addition, subepithelial serous glands in the nasolacrimal passage revealed positive intracytoplasmics reactivity of the acinar cells and the cells lining the excretory duct system of the glands (Fig. 2H). Respiratory epithelium from the nose (positive control): Positivity of PLUNC occurred intracytoplasmically in the double-layered respiratory epithelium (exception: goblet cells) and strong reactivity was visible at the surface of the cells (Fig. 2I).

Enzyme-linked immunosorbent assay revealed mean values of PLUNC concentration in lacrimal gland 0.355 ng/mg ($n = 4$), in conjunctiva 0.529 ng/mg ($n = 3$), in eyelid of 0.575 ng/mg ($n = 2$), and cornea 2.202 ng/mg ($n = 3$) (Fig. 3A).

The PLUNC Concentration Is Significantly Increased in Tears of Patients Suffering From Different Types of DED

Quantification of PLUNC in tears of patient suffering from ADDE revealed a mean value concentration of 0.41 ng/mg ($n = 11$), whereas patients with the hyperevaporative form (EDE) demonstrated 0.17 ng/mg ($n = 22$, $P < 0.005$). With that, the PLUNC concentration is significantly higher in both dry eye forms compared with tears from healthy volunteers (0.02 ng/mg; $n = 16$) (Fig. 3B).

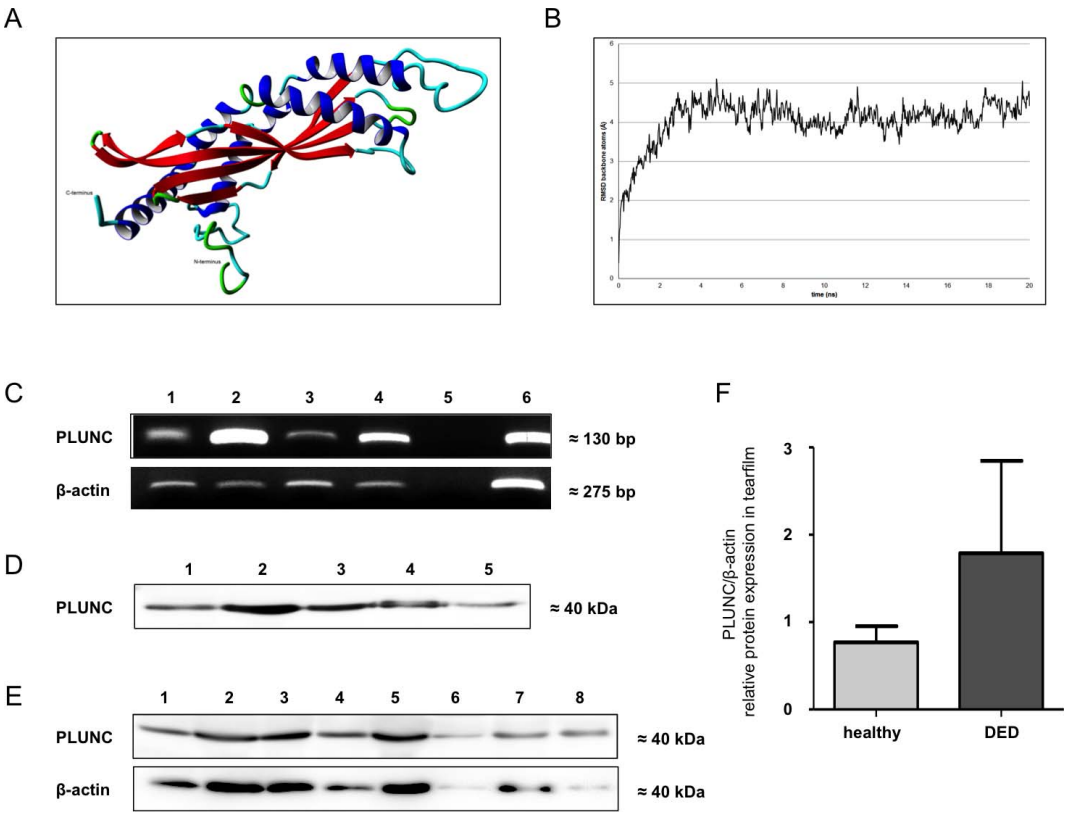

Figure 1. Molecular–biological detection and structural characterization of PLUNC. (**A**) Three-dimensional structure model of PLUNC (only the protein backbone is shown), *blue*: α-helices, *red*: β-sheets, *cyan/green*: turns and random elements. (**B**) The PLUNC model stability test via 20 ns molecular dynamics simulation. Only minor fluctuations in the RMSD plot for the protein backbone atoms indicate a stable protein structure model. (**C**) Expression of specific PLUNC mRNA amplification products. The following samples were used: lacrimal gland [1], eyelid [2], conjunctiva [3], cornea [4]. The negative control without template cDNA [5], and the positive control – lung DNA [6]. (**D**) Western blot analysis with anti-PLUNC antibody from lacrimal gland [1] eyelid [2], conjunctiva [3], cornea [4]. (**E**) Western blot analysis with anti-PLUNC antibody from tear film sample [1–5] without DED and with DED [6–7] the positive control – lung [8]. (**F**) Semiquantification of tear film samples with and without DED.

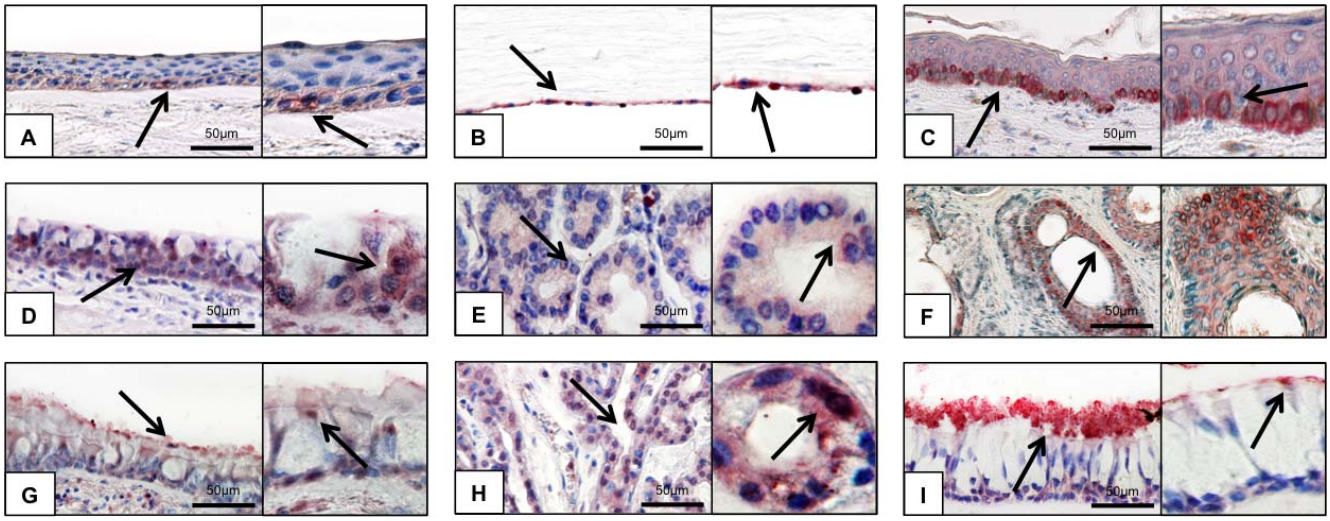

Figure 2. Immunohistochemical detection of PLUNC in in tissue of the tear system. (**A**) Cornea: protein detected in the basal epithelium. (**B**) Cornea endothelia: positive staining only in the epithelial cells. (**C**) Eyelid: PLUNC was detected in the basal epithelium of the eyelid. (**D**) Conjunctiva: multilayer epithelium of the conjunctiva shows weak reactivity. (**E**) Lacrimal gland: intracytoplasmically within acinar cells. (**F**) Meibomian glands: PLUNC detected intracytoplasmatically within acinar cells and the excretory duct system. (**G**, **H**) Epithelium of the efferent tear ducts: intracytoplasmatically within epithelial cells (7) and protein distribution as a superficial layer (8). (**I**) Bronchial epithelia: cytoplasmic protein distribution in bronchioles and as a superficial layer, lung tissue used as positive control. Insets show magnifications. *Scale bars*: [1–6] 50 µm. *Red staining* indicates positive reaction.

Investigative Ophthalmology & Visual Science

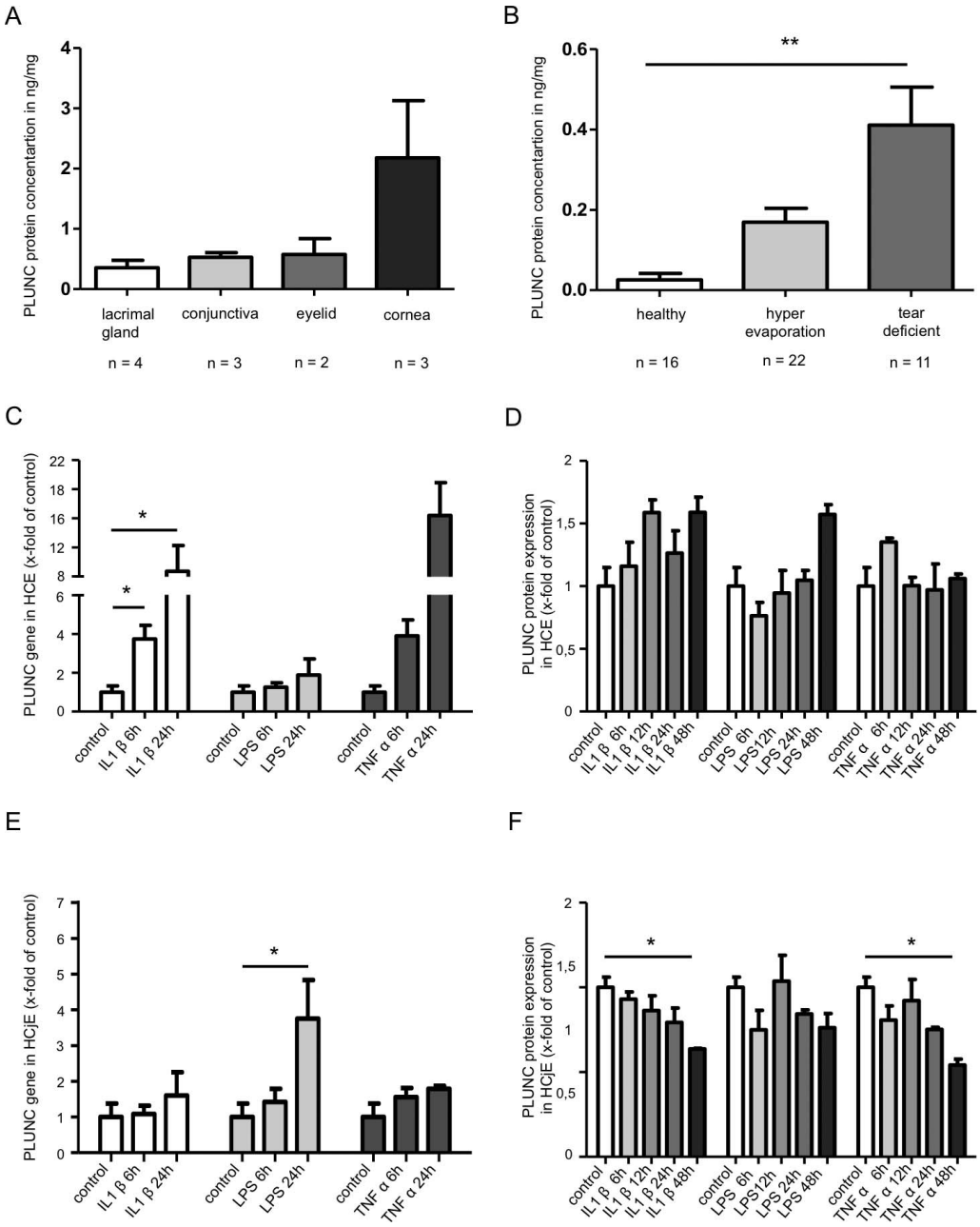

FIGURE 3. Quantification of PLUNC. (**A**) Quantification of PLUNC in lacrimal gland tissue ($n = 4$), conjunctiva ($n = 3$), and eyelid ($n = 2$) by ELISA. Mean values of lacrimal gland: 0.355 ng/mg, conjunctiva: 0.529 ng/mg and in eyelid: 0.575 ng/mg. (**B**) Quantification of PLUNC in tear film by ELISA. Mean values of healthy: 0.007 ng/mg, hyperevaporation: 0.17 ng/mg and in tear deficient: 0.41 ng/mg. (**C**) Real-time RT-PCR of PLUNC: Stimulation of HCE cells for 0, 6, and 24 hours with 10 ng/mL of recombinant IL-1β, TNFα, and 100 ng/mL LPS. (**D**) ELISA of PLUNC: Stimulation of HCE cells for 0, 6, and 24 hours with 10 ng/mL of recombinant IL-1β, TNFα, and 100 ng/mL LPS. (**E**) Real-time RT-PCR of PLUNC: Stimulation of HCjE cells for 0, 6, and 24 hours with 10 ng/mL of recombinant IL-1β, TNFα, and 100 ng/mL LPS. (**F**) ELISA of PLUNC: Stimulation of HCjE cells for 0, 6, and 24 hours with 10 ng/mL of recombinant IL-1β, TNFα, and 100 ng/mL LPS. Statistical significance ($n = 3$; $^{*}P \leq 0.05$, $^{**}P \leq 0.005$). The regulation of PLUNC transcript levels was expressed as mean ± SEM.

Cytokines and Bacterial Supernatants Have Slight Effects on the PLUNC Expression by Cultivated HCE and HCjE

Human cornea epithelial (HCE) and conjunctivial epithelial cell line (HCjE) were used and cultivated to investigate whether PLUNC is regulated by proinflammatory cytokines and bacterial supernatants. Both cell lines are well established and known to produce surfactant proteins after stimulation with bacterial supernatants. After stimulation with IL-1β or TNFα, an upregulation of PLUNC expression could be observed in HCE after real-time PCR analysis (Fig. 3C). Stimulation with LPS revealed no significant effect. In contrast, stimulation with LPS showed a significantly upregulation in HCjE, whereas in this cell line, IL-1β and TNFα demonstrated no effect (Fig. 3D). A significant upregulation in the PLUNC mRNA expression could be detected after stimulation with bacterial supernatants of EC, but not with PA in HCE cells (Fig. 4A). The PA had a slight effect on the PLUNC expression after 6-hour stimulation time in HCjE cells, whereas EC had no effect

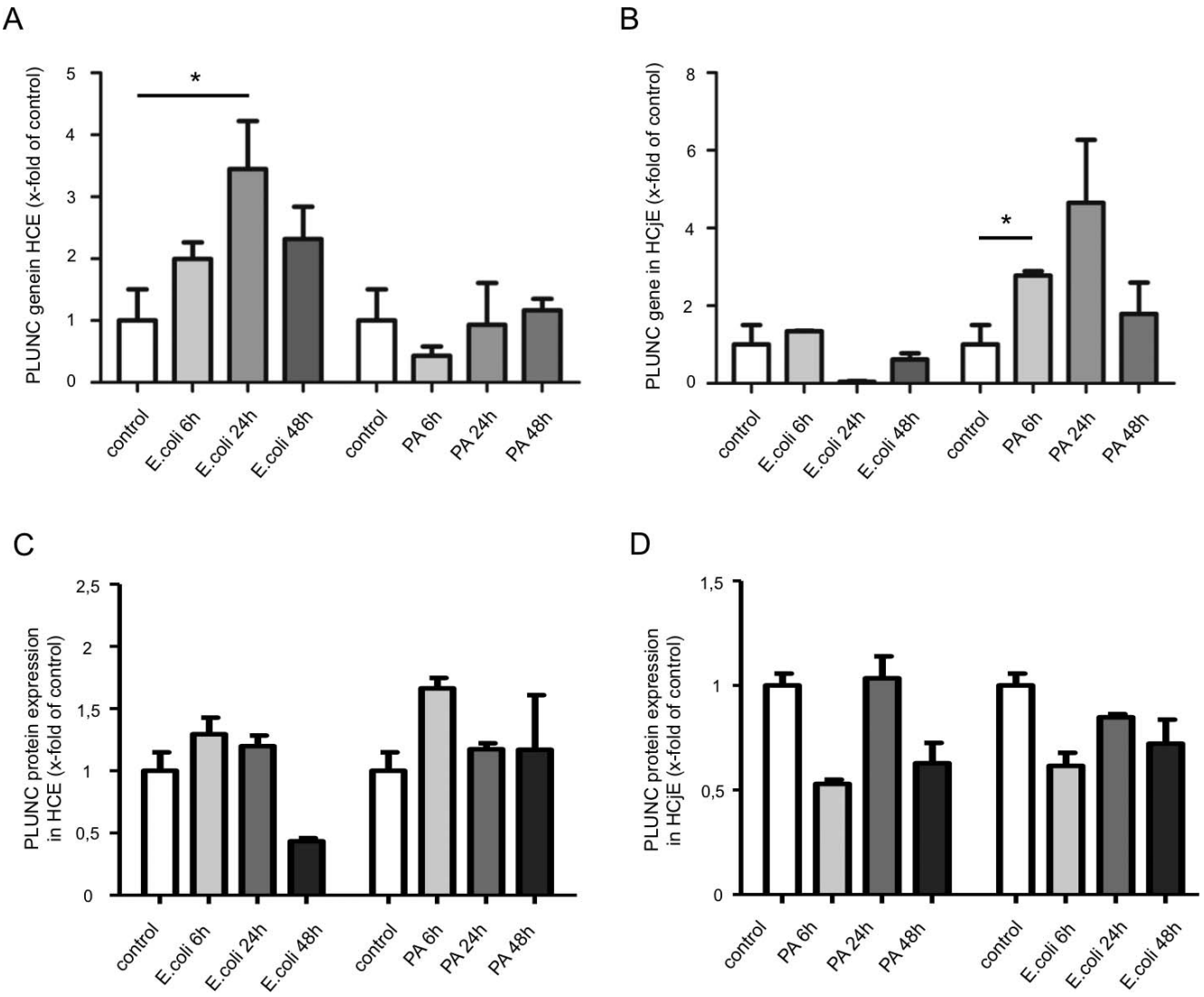

FIGURE 4. In vitro stimulation with bacterial supernatants. Real-time RT-PCR of PLUNC: Stimulation of HCE cells (**A**) and HCjE cells (**C**) for 6, 24, and 48 hours with bacterial supernatant of *Escherichia coli* (E. coli) and *Pseudomonas aeruginosa* (PA). ELISA of PLUNC: Stimulation of HCE cells (**B**) and HCjE cells (**D**) for 6, 24, and 48 hours with bacterial supernatant of E. coli and PA. Statistical significance ($n = 3$; $^*P \leq 0.05$). The regulation of PLUNC transcript levels was expressed as mean ± SEM.

in this case (Fig. 4B). Enzyme-linked immunosorbent assay indicated that none of the stimulants (IL-1β, LPS, TNFα, EC, PA) had any significant effect on the PLUNC protein concentration in HCE cells (Figs. 3D, 4C). In HCjE cells, IL-1β and TNFα significantly reduced the PLUNC concentration over time, whereas LPS and supernatants of EC and PA had no effect (Figs. 3F, 4D).

Protein–Lipid MD Simulations Reveal That PLUNC Interacts With Model Lipids

In all five performed simulations where the protein model was placed in vicinity to the DPPC bilayer model system (orientations 1–5), the PLUNC structure model approached the layer surface in less than 40 ns and started to interact with the polar lipid head groups. Only in one case, this process took nearly 60 ns. The two simulations with imposed N-terminal transmembrane section (orientations 6 and 7) showed no major changes in protein position or orientation. The transmembrane region remained intact, hydrogen bonds and electrostatic interactions were established very quickly to stabilize the protein model on the membrane surface. All seven orientations showed no unfolding or loss of secondary structure elements during the simulation and the influence of the protein contact on the area per lipid value was mainly negligible. However, the progression of the RMSD and protein-lipid interaction energy over the simulation time as well as the interaction energy of the last simulation snapshot allowed discrimination between different orientations. From all performed simulations, the orientations 2 and 7 showed the best results in RMSD and protein–lipid interaction energy. The final protein position in these two orientations was very similar, with the model located parallel to the membrane surface and nearly the same protein parts contributing to the contact surface between protein and lipids. For orientation 2 (Fig. 5A), the protein was bound to the lipid surface mostly by various hydrogen bonds between amino acids and the lipid head groups as well as ionic interactions. This was sufficient for a stable fixation of the protein during the MD. Although the presence of the protein formed a flat hollow on the membrane surface where it resisted, no protein parts extended into the hydrophobic region of the membrane and the carbon chain

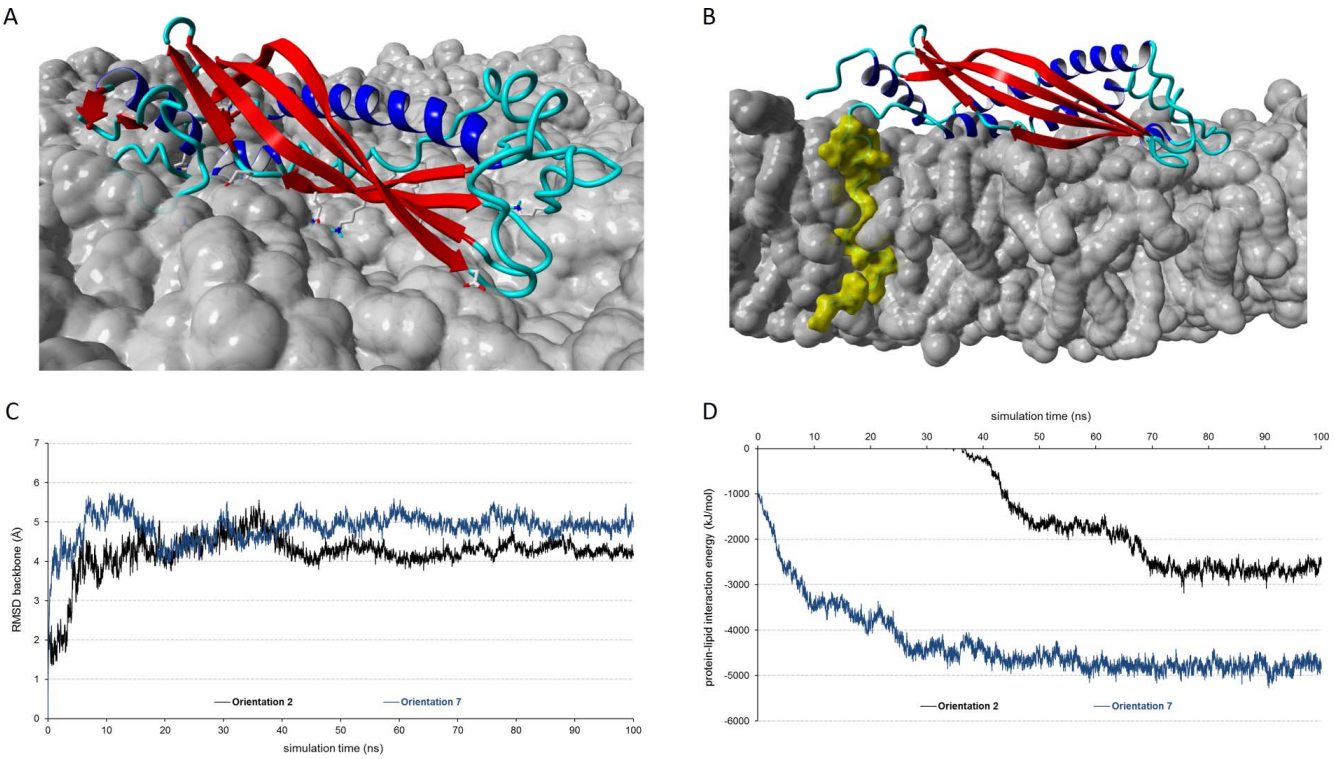

Figure 5. The 100-ns protein–lipid MD simulation results. (**A**) Last snapshot of the MD with orientation 2. The membrane is shown as *gray surface*, the PLUNC protein in secondary structure only representation (α-helix in *blue*, β-sheet in *red*, coil in *cyan*). Amino acid side chains shown in stick representation (without aliphatic hydrogens) interact with the lipids by hydrogen bonds or ionic interactions. (**B**) Last snapshot of the MD with orientation 7. The membrane is shown as *gray surface*, the PLUNC protein in secondary structure only representation (α-helix in *blue*, β-sheet in *red*, coil in *cyan*). The membrane system was cut perpendicularly to show the immersion of the protein into the head group region and the penetration of the N-terminus through the membrane (*yellow surface*). (**C**) Plot of the backbone atoms RMSD (in Å) for the 100-ns MD simulations of orientation 2 (*black*) and orientation 7 (*blue*). (**D**) Plot of the interaction energy (in kJ/mol) between PLUNC and lipids according to force-field parameters for the 100-ns MD simulations of orientation 2 (*black*) and orientation 7 (*blue*).

ordering remained unaffected. The protein in orientation 7 (Fig. 5B) showed nearly the same position as in orientation 2 and the amino acids responsible for the protein–lipid interactions were comparable. The only difference was the N-terminus, which was modeled with a kink between position 23 and 24, so that the residues 1 to 22 penetrated the membrane. Hydrogen bonds to the lipid head groups by the residues 16 and 18 on the protein side as well as position 1 and 11 on the opposite side of the membrane stabilized the transmembrane region on either end. This fixation of the protein seemed to enhance the interactions between protein and polar head groups. But again, no protein parts influenced or interacted with the hydrophobic membrane core. Not even the inserted N-terminus induced any visible or measurable influence on the lipid chains. The RMSD curves (Fig. 5C, orientation 2 in black, orientation 7 in blue) for both models showed that the protein structures needed approximately 40 ns to accommodate to the environment. During this time period, the model in orientation 2 was freely rotating in the water phase until the protein–lipid contact was established. For orientation 7, a loose contact on the membrane surface was already present at the simulation start and the tightening of the interactions during the simulation caused RMSD fluctuations. Both protein models could be considered as equilibrated after 50 ns. The force field energy for the protein–lipid interaction also showed the equilibration of both systems. For orientation 2 (Fig. 5D, black plot), the interaction energy raised quickly after the first contact at 40 ns, reaching a plateau between 50 and 70 ns, to a value of approximately 2600 kJ/mol where it remained stable until the end of the simulation. Orientation 7 showed an interaction energy of approximately 1000 kJ/mol already at simulation start (Fig. 5D, blue plot), the final level of approximately 4800 kJ/mol was reached after 55 ns without notable fluctuations thereafter. This indicated that the modeling of a transmembranal N-terminus for PLUNC nearly doubled the protein–lipid interaction energy in comparison to a similar scenario without transmembrane section in a MD simulation.

Discussion

Molecular modeling and simulation offer great tools to support the initial characterization of a protein and to obtain first insights into its function. As a prerequisite for these techniques, detailed information about the three-dimensional protein structure are necessary, as found in public databases in terms of x-ray or NMR data. Unfortunately, there was no three-dimensional structure available for PLUNC at the beginning of this work. Therefore, homology modeling was performed to produce a protein structure model for PLUNC. This model showed a very good overall quality and was generated based on the x-ray structure of latherin, a PLUNC family member with similar predicted fold.[28] This final PLUNC model was used for all further modeling experiments presented in this work.

During conduction of our investigations, x-ray structures for PLUNC were published[44] (PDB codes "4KGH" and "4KGO"). A structural alignment of the final PLUNC model and the x-ray structure of "4KGH" revealed a high structure similarity, indicated by the low RMSD value of 1660 Å. Moreover, our

model includes the N-terminal residues 1 to 23 and various loop regions (57–88, 149–153), which are not part of the published x-ray structure due to high flexibility. Therefore, the full-length PLUNC model obtained in this work is more suitable for simulation studies than the incomplete x-ray structure.

The PLUNC gene was first demonstrated in developing nasal epithelium, adult trachea, and bronchi.[45] Translation of the gene leads to the formation of the SPLUNC protein, initially detected as a secretory product in the sputum and the secretions of the tracheobronchial epithelium.[46] We here show that PLUNC is also part of the ocular surface system. It is not only produced by different structures of the ocular surface and lacrimal apparatus such as lacrimal gland, cornea, conjunctiva, meibomian gland, glands of Moll, and the epithelium of the efferent tear ducts, but is also secreted into the tear fluid. The findings obtained also confirm that the two immortalized cell lines used in our study (HCE and HCjE) for further stimulation experiments produce and secrete PLUNC and therefore are useful as model to study PLUNC regulation at the ocular surface. The PLUNC is synthesized in particular by acinar cells of the lacrimal gland, the conjunctival epithelial cells, with the exception of goblet cells, and the epithelial cells of the efferent tear duct system (again with the exception of goblet cells) and passes into the tear film as a secretory product. This is consistent with the findings of investigations of PLUNC detection in the epithelium and the glands of the respiratory tract. In contrast, immunoreactivity is detected in the cornea only in the basal epithelial cells and corneal endothelium. This leads to the assumption that the PLUNC produced in the basal epithelial cells is not secreted, and thus is not released into the tear film, but rather serves some other function. An important immune defense-related role of PLUNC is well documented in the lungs,[47] where PLUNC can prevent, for example, infection with *Klebsiella pneumonia*.[48] Also, PLUNC can influence pulmonary fluid regulation by way of sodium channel (ENaC) inhibition.[11] Because the cornea is also an organ the fluid balance of which must be regulated very precisely due to its transparency, the fact that PLUNC is only detected in the basal epithelial cells and corneal endothelium could also indicate that PLUNC is involved in fluid regulation here. In this context, the interaction with the β-subunit of the ENaC channel, which is expressed in the endothelial cells and the basal epithelial cells of the corneal limbus but is not detectable in the overlying epithelial layers, could be important.[49] So far, however, which of the four known subunits of ENaC channel SPLUNC can interact with is not known and must be clarified by further investigation.

A further insight based on these findings is that PLUNC is also formed by meibocytes and the epithelial cells of the excretory ducts of the meibomian glands. Presumably, PLUNC is integrated in the meibocytes in the course of their transformation into the secretion of the meibomian glands. It has been clearly established that meibocytes produce different proteins that interact with the lipids of meibum.[50] Interestingly, in this context, the evidence shows that DED patients suffering from meibomian gland dysfunction (MGD) also have raised PLUNC concentrations. Less meibum with an additional change in viscosity is formed in these patients, so that the increased PLUNC concentration is rather surprising. There are two conceivable hypotheses for this: (1) More tears and PLUNC are produced in reaction to increased evaporation in the absence of the protective lipid layer of the tear film in MGD, whereupon more PLUNC is excreted by the lacrimal gland and conjunctiva due to its immunologic function and to regulate the fluid balance of the ocular surface, resulting in a higher concentration of PLUNC in the tear fluid. This could also explain why the concentration of PLUNC is even higher in aqueous tears deficit (ADDE), as more PLUNC is produced reactively to protect the epithelial barrier. (2) A second conceivable reason for the raised PLUNC concentration in the tear film is that the relative volume of liquid is greatly reduced in the tear film and therefore the proportion of the components of the tear film has shifted in favor of PLUNC protein or other proteins.

In patients with the hypovolemic form of dry eye (ADDE) and also in the evaporative form (EDE), PLUNC concentration in the tear film is increased many times over. These patients with ADDE in particular show a quantitative reduction of the aqueous phase of the tear film.[51] As described above, PLUNC can bind to epithelial sodium channels and presumably influences the regulation of tear fluid volume by inhibiting them as has been shown in the lung.[11] Since the hypovolemic form of dry eye (EDE) is characterized by a quantitative tear fluid deficit with tear film break-up, this could be a further explanatory mechanism for understanding DED. The epithelial sodium channels (ENaC) play an important sensory function in the ocular system as nociceptors.[52] Considering that approximately 70% of total nerve fibers in the cornea are stimulated by mechanical, chemical, and thermal stimuli,[53] a relevant regulatory mechanism for tear film production can be ascribed to the sensory corneal nerves. This is evident in patients with familial dysautonomia (Riley-Day syndrome). This is a genetically conditioned malfunction of the autonomic nervous system potentially involving, inter alia, denervation of the cornea.[54] Due to the permanent corneal anesthesia, the patients develop a special form of dry eye due to lack of tear production. This pathophysiologic mechanism suggests that the role played by PLUNC in regulation of the tear film could involve a neuronal pathway in addition to direct receptor-mediated fluid regulation. What is not yet clear is whether the neuronal influence of PLUNC induces a protective effect on the ocular system or contributes to diseases such as DED or inflammatory processes due to protein-related dysregulation of the neuronal system.

The innate immune defense system at the ocular surface effectively prevents pathogenic colonization of the ocular surface epithelia, thereby making a significant contribution to maintenance of visual perception. The humoral system comprising numerous antimicrobial peptides and proteins such as lysozyme, lactoferrin, lipocalin, defensins, and Psoriasin is an essential component of the innate immune defense system.[55–57] It has been demonstrated that the surfactant proteins SP-A and SP-D also make functional contributions to the immune system. Both nonspecific and specific immune defense functions are ascribed to them,[58] whereby the mechanism of action of the two surfactant proteins differs.[59]

The present results show that PLUNC is also a synthesized surfactant protein like the surfactant proteins SP-A and -D already confirmed at the ocular surface and in the lacrimal apparatus.[2,3] The PLUNC is produced at the ocular surface and in the lacrimal apparatus, with the exception of the cornea, by the same cells that produce SP-A and SP-D.[2] In contrast to SP-A and SP-D, the activity of PLUNC also involves a significant reduction in surface tension (at least in the respiratory tract), apparently resulting in "anti-biofilm activity."[48] Also, PLUNC can directly inhibit bacterial growth and influence the activity of neutrophils, the role of which is particularly important when the eyes are closed,[60] and promote mucociliary clearance.[48] The contributing mechanisms are, however, not yet fully understood and many of the results were obtained in transgenic mice.

The findings, which were collected in vitro, demonstrate that both cell lines (HCE and HCjE) synthesize PLUNC. Stimulations with bacterial cell wall components (LPS), bacterial supernatants of *E. coli* and *P. aeruginosa* laboratory strains and with proinflammatory cytokines IL-1β and TNFα,

were followed by partially significant induction of gene expression of PLUNC in HCE and HCjE. However, this induction was not coupled with an increased PLUNC protein synthesis in all cases. In vivo PLUNC is not equally produced by all epithelial cellular layers of the cornea. Future studies, for example, with pathogenic bacteria from ocular surface isolates will have to clarify whether PLUNC is actively involved in immune defense at the ocular surface, acts only against specific pathogens, or exerts a broader antimicrobial function.

Of interest, PLUNC shows sequential and structural identities to the other two known SPs B and C,[29] both of which have also been shown to be produced and secreted at the ocular surface and in the lacrimal apparatus.[48] Due to the pronounced hydrophobicity of the protein, PLUNC is classified with them in the group of hydrophobic surfactant proteins.[7] Along with SP-B and SP-C, which occur only in small amounts in upper respiratory tract secretion,[6] PLUNC is considered an additional factor reducing surface tension in the lungs. Simulations with the final PLUNC model performed in the present work revealed that a slight instability of PLUNC in an aqueous environment is mainly induced by a flexible N-terminus and single loops with a high density of hydrophobic amino acids, as indicated by the high overall content of hydrophobic residues known from the literature.[61] These protein parts would be stabilized by the interaction with a lipid membrane, as demonstrated by MD simulations for the N-terminus. In general, our MD simulations showed that PLUNC is indeed able to interact with a lipid system. The hydrophobic N-terminus may determine the final orientation of the protein on the membrane surface and also the interaction strength. Although the obtained force-field values can only give a rough estimation of in vivo interaction energies, they already indicate the high potential of PLUNC to interact with a membrane system. This represents a shared feature with already known surfactant proteins like SP-B and SP-C, additionally justifying the association of PLUNC to this family of proteins.

In summary, we have detected and characterized PLUNC within the human ocular surface system, lacrimal apparatus, and in human cornea and conjunctiva cell lines HCE and HCjE, and have demonstrated first functional and pathologic features in vivo and in vitro. The findings indicate the high potential of PLUNC to interact with a membrane system. This represents a shared feature with already known surfactant proteins like SP-B and SP-C, justifying the association of PLUNC to this family of proteins and supporting the hypothesis that PLUNC is active in reducing surface tension of the tear film. Moreover, interaction of PLUNC with ENaC channels is possible, suggesting that it also plays a role in fluid balance regulation at the ocular surface. All generated findings are very interesting; however, they raise more questions than they answer and so far only allow speculation. The importance of PLUNC, especially in various diseases of the ocular surface, will thus require more detailed characterization in further studies.

Acknowledgments

The authors thank Hong Nguyen, Anke Fischer, Elke Kretschmar, Jessica Braun, and Maike Hemmerlein for excellent technical assistance.

Supported by the German Research Foundation (DFG, Program Grants BR1329/12-1, BR 3681/2-1, and PA738/9-2), the Ernst und Berta Grimmke Stiftung (Program Grant 1/15), and the Sicca Forschungsförderung of the Professional Association of German Ophthalmologists. MS obtained a travel award from the Tear Film and Ocular Surface Society to the 7th International Tear Film and Ocular Surface Conference in Taormina/Sicily/Italy in 2013 for his presentation: "PLUNC, a new surfactant protein of the tear film."

Disclosure: **M. Schicht**, None; **F. Rausch**, None; **M. Beron**, None; **C. Jacobi**, None; **F. Garreis**, None; **N. Hartjen**, None; **S. Beileke**, None; **F. Kruse**, None; **L. Bräuer**, None; **F. Paulsen**, None

References

1. McDermott AM. Defensins and other antimicrobial peptides at the ocular surface. *Ocul Surf*. 2004;2:229–247.
2. Bräuer L, Kindler C, Jäger K, et al. Detection of surfactant proteins A and D in human tear fluid and the human lacrimal system. *Invest Ophthalmol Vis Sci*. 2007;48:3945–3953.
3. Bräuer L, Johl M, Börgermann J, Pleyer U, Tsokos M, Paulsen FP. Detection and localization of the hydrophobic surfactant proteins B and C in human tear fluid and the human lacrimal system. *Curr Eye Res*. 2007;32:931–938.
4. Ni M, Evans DJ, Hawgood S, Anders EM, Sack RA, Fleiszig SMJ. Surfactant protein D is present in human tear fluid and the cornea and inhibits epithelial cell invasion by *Pseudomonas aeruginosa*. *Infect Immun*. 2005;73:2147–2156.
5. Bernhard W, Haagsman HP, Tschernig T, et al. Conductive airway surfactant: surface-tension function, biochemical composition, and possible alveolar origin. *Am J Respir Cell Mol Biol*. 1997;17:41–50.
6. Khoor A, Stahlman MT, Gray ME, Whitsett JA. Temporal-spatial distribution of SP-B and SP-C proteins and mRNAs in developing respiratory epithelium of human lung. *J Histochem Cytochem*. 1994;42:1187–1199.
7. Bartlett JA, Gakhar L, Penterman J, et al. PLUNC: a multifunctional surfactant of the airways. *Biochem Soc Trans*. 2011;39:1012–1016.
8. Bingle L, Cross SS, High AS, et al. SPLUNC1 (PLUNC) is expressed in glandular tissues of the respiratory tract and in lung tumours with a glandular phenotype. *J Pathol*. 2005;205:491–497.
9. Tsou YA, Peng MT, Wu YF, et al. Decreased PLUNC expression in nasal polyps is associated with multibacterial colonization in chronic rhinosinusitis patients. *Eur Arch Otorhinolaryngol*. 2014;271:299–304.
10. Lukinskiene L, Liu Y, Reynolds SD, et al. Antimicrobial activity of PLUNC protects against *Pseudomonas aeruginosa* infection. *J Immunol*. 2011;187:382–390.
11. Garcia-Caballero A, Rasmussen JE, Gaillard E, et al. SPLUNC1 regulates airway surface liquid volume by protecting ENaC from proteolytic cleavage. *Proc Natl Acad Sci U S A*. 2009;106:11412–11417.
12. Passali D, Sarafoleanu C, Manea C, et al. PLUNC proteins positivity in patients with chronic rhinosinusitis: a case-control study. *ScientificWorldJournal*. 2014;2014:853583.
13. Sung YK, Moon C, Yoo JY, et al. Plunc, a member of the secretory gland protein family, is up-regulated in nasal respiratory epithelium after olfactory bulbectomy. *J Biol Chem*. 2002;277:12762–12769.
14. Bingle L, Wilson K, Musa M, et al. BPIFB1 (LPLUNC1) is upregulated in cystic fibrosis lung disease. *Histochem Cell Biol*. 2012;138:749–758.
15. DEWS-Report. The definition and classification of dry eye disease: report of the Definition and Classification Subcommittee of the International Dry Eye WorkShop (2007). *Ocul Surf*. 2007;5:75–92.
16. Schiffman RM, Christianson MD, Jacobsen G, Hirsch JD, Reis BL. Reliability and validity of the Ocular Surface Disease Index. *Arch Ophthalmol*. 2000;118:615–621.
17. Jacobi C, Jacobi A, Kruse FE, Cursiefen C. Tear film osmolarity measurements in dry eye disease using electrical impedance technology. *Cornea*. 2011;30:1289–1292.
18. Höh H, Schirra F, Kienecker C, Ruprecht KW. Lid-parallel conjunctival folds are a sure diagnostic sign of dry eye [in German]. *Ophthalmolog*. 1995;92:802–808.

19. Tomlinson A, Khanal S. Assessment of tear film dynamics: quantification approach. *Ocul Surf*. 2005;3:81–95.
20. Posa A, Brauer L, Schicht M, Garreis F, Beileke S, Paulsen F. Schirmer strip vs. capillary tube method: non-invasive methods of obtaining proteins from tear fluid. *Ann Anat*. 2012;195:137–142.
21. Araki-Sasaki K, Ohashi Y, Sasabe T, et al. An SV40-immortalized human corneal epithelial cell line and its characterization. *Invest Ophthalmol Vis Sci*. 1995;36:614–621.
22. Diebold Y, Calonge M, Enriquez de Salamanca A, et al. Characterization of a spontaneously immortalized cell line (IOBA-NHC) from normal human conjunctiva. *Invest Ophthalmol Vis Sci*. 2003;44:4263–4274.
23. Bräuer L, Schicht M, Stengl C, et al. Detection of surfactant proteins A, B, C and D in human gingiva and saliva. *Biomed Tech (Berl)*. 2012;57:59–64.
24. Schicht M, Knipping S, Hirt R, et al. Detection of surfactant proteins A, B, C, and D in human nasal mucosa and their regulation in chronic rhinosinusitis with polyps. *Am J Rhinol Allergy*. 2013;27:24–29.
25. Krieger E, Darden T, Nabuurs SB, Finkelstein A, Vriend G. Making optimal use of empirical energy functions: force-field parameterization in crystal space. *Proteins*. 2004;57:678–683.
26. Krieger E, Joo K, Lee J, et al. Improving physical realism, stereochemistry, and side-chain accuracy in homology modeling: four approaches that performed well in CASP8. *Proteins*. 2009;77:114–122.
27. Consortium U. Reorganizing the protein space at the Universal Protein Resource (UniProt). *Nucleic Acids Res*. 2012;40:D71–D75.
28. Vance SJ, McDonald RE, Cooper A, Smith BO, Kennedy MW. The structure of latherin, a surfactant allergen protein from horse sweat and saliva. *J R Soc Interface*. 2013;10:20130453.
29. Gakhar L, Bartlett JA, Penterman J, et al. PLUNC is a novel airway surfactant protein with anti-biofilm activity. *PLoS One*. 2010;5:e9098.
30. Laskowski RA, MacArthur DS, Moss DS, Thornton JM. PROCHECK: a program to check the stereochemical quality of protein structures. *J Appl Cryst*. 1993;26:283–291.
31. Sippl MJ. Recognition of errors in three-dimensional structures of proteins. *Proteins*. 1993;17:355–362.
32. Duan Y, Wu C, Chowdhury S, et al. A point-charge force field for molecular mechanics simulations of proteins based on condensed-phase quantum mechanical calculations. *J Comput Chem*. 2003;24:1999–2012.
33. Kabsch W, Sander C. Dictionary of protein secondary structure: pattern recognition of hydrogen-bonded and geometrical features. *Biopolymers*. 1983;22:2577–2637.
34. Sommer B, Dingersen T, Gamroth C, et al. CELLmicrocosmos 2.2 MembraneEditor: a modular interactive shape-based software approach to solve heterogeneous membrane packing problems. *J Chem Inf Model*. 2011;51:1165–1182.
35. Hess B, Kutzner C, van der Spoel D, Lindahl E. GROMACS 4: algorithms for highly efficient, load-balanced, and scalable molecular simulation. *J Chem Theory Comput*. 2008;4:435–447.
36. Oostenbrink C, Villa A, Mark AE, van Gunsteren WF. A biomolecular force field based on the free enthalpy of hydration and solvation: the GROMOS force-field parameter sets 53A5 and 53A6. *J Comput Chem*. 2004;25:1656–1676.
37. Kukol A. Lipid models for united-atom molecular dynamics simulations of proteins. *J Chem Theory Comput*. 2009;5:615–626.
38. Hoover WG. Canonical dynamics: equilibrium phase-space distributions. *Phys Rev A*. 1985;31:1695–1697.
39. Nosé S. A molecular dynamics method for simulations in the canonical ensemble. *Mol Phys*. 1984;52:255–268.
40. Parrinello M, Rahman A. Polymorphic transitions in single crystals: a new molecular dynamics method. *J Appl Phys*. 1981;52:7182–7190.
41. Hess B, Bekker H, Berendsen HJC, Fraaije JGEM. LINCS: a linear constraint solver for molecular simulations. *J Comput Chem*. 1997;18:1463–1472.
42. Essmann U, Perera L, Berkowitz ML, Darden T, Lee H, Pedersen LG. A smooth particle mesh Ewald method. *J Chem Phys*. 1995;103:8577–8593.
43. Humphrey W, Dalke A, Schulten K. VMD: visual molecular dynamics. *J Mol Graph*. 1996;14:33–38, 27–38.
44. Garland AL, Walton WG, Coakley RD, et al. Molecular basis for pH-dependent mucosal dehydration in cystic fibrosis airways. *Proc Natl Acad Sci U S A*. 2013;110:15973–15978.
45. Weston WM, LeClair EE, Trzyna W, et al. Differential display identification of plunc, a novel gene expressed in embryonic palate, nasal epithelium, and adult lung. *J Biol Chem*. 1999;274:13698–13703.
46. LeClair EE, Nguyen L, Bingle L, et al. Genomic organization of the mouse plunc gene and expression in the developing airways and thymus. *Biochem Biophys Res Commun*. 2001;284:792–797.
47. Di YP. Functional roles of SPLUNC1 in the innate immune response against gram-negative bacteria. *Biochem Soc Trans*. 2011;39:1051–1055.
48. Liu Y, Bartlett JA, Di ME, et al. SPLUNC1/BPIFA1 contributes to pulmonary host defense against *Klebsiella pneumoniae* respiratory infection. *Am J Pathol*. 2013;182:1519–1531.
49. Krueger B, Schlotzer-Schrehardt U, Haerteis S, et al. Four subunits (alphabetagammadelta) of the epithelial sodium channel (ENaC) are expressed in the human eye in various locations. *Invest Ophthalmol Vis Sci*. 2012;53:596–604.
50. Green-Church KB, Butovich I, Willcox M, et al. The international workshop on meibomian gland dysfunction: report of the subcommittee on tear film lipids and lipid-protein interactions in health and disease. *Invest Ophthalmol Vis Sci*. 2011;52:1979–1993.
51. Nichols JJ, Sinnott LT. Tear film, contact lens, and patient factors associated with corneal staining. *Invest Ophthalmol Vis Sci*. 2011;52:1127–1137.
52. Hwang SW, Oh U. Current concepts of nociception: nociceptive molecular sensors in sensory neurons. *Curr Opin Anaesthesiol*. 2007;20:427–434.
53. Belmonte C, Aracil A, Acosta MC, Luna C, Gallar J. Nerves and sensations from the eye surface. *Ocul Surf*. 2004;2:248–253.
54. George L, Chaverra M, Wolfe L, et al. Familial dysautonomia model reveals Ikbkap deletion causes apoptosis of Pax3+ progenitors and peripheral neurons. *Proc Natl Acad Sci U S A*. 2013;110:18698–18703.
55. McDermott AM. The role of antimicrobial peptides at the ocular surface. *Ophthalmic Res*. 2009;41:60–75.
56. Garreis F, Gottschalt M, Paulsen FP. Antimicrobial peptides as a major part of the innate immune defense at the ocular surface. *Dev Ophthalmol*. 2010;45:16–22.
57. Garreis F, Gottschalt M, Schlorf T, et al. Expression and regulation of antimicrobial peptide psoriasin (S100A7) at the ocular surface and in the lacrimal apparatus. *Invest Ophthalmol Vis Sci*. 2011;52:4914–4922.
58. Schicht M, Posa A, Paulsen F, Brauer L. The ocular surfactant system and its relevance in the dry eye [in German]. *Klin Monbl Augenheilkd*. 2010;227:864–870.
59. Crouch E, Wright JR. Surfactant proteins a and d and pulmonary host defense. *Ann Rev Physiol*. 2001;63:521–554.
60. Sack RA, Conradi L, Krumholz D, Beaton A, Sathe S, Morris C. Membrane array characterization of 80 chemokines, cytokines, and growth factors in open- and closed-eye tears: angiogenin and other defense system constituents. *Invest Ophthalmol Vis Sci*. 2005;46:1228–1238.
61. McDonald RE, Fleming RI, Beeley JG, et al. Latherin: a surfactant protein of horse sweat and saliva. *PLoS One*. 2009;4:e5726.

Investigative Ophthalmology & Visual Science